Formation of Bubbles in a Multisection Flow-Focusing Junction

Formation of Bubbles in a Multi-section Flow-focusing Junction

Michinao Hashimoto and George M. Whitesides*

Department of Chemistry and Chemical Biology, Harvard University

12 Oxford St., Cambridge, MA, 02138, U.S.A.

Journal: Small

[*] To whom correspondence may be addressed: gwhitesides@gmwgroup.harvard.edu

Abstract

This paper described the formation of bubbles in a flow-focusing (FF) junction comprising multiple rectangular sections. The simplest junctions comprised two sections (*throat* and *orifice*). Systematic investigation of the influence of the flow of liquid, and of the geometry of the junction, on the formation of bubbles identified regimes that generated monodisperse, bidisperse, and tridisperse trains of bubbles. Mechanisms by which these junctions formed monodisperse and bidisperse bubbles were inferred from the shapes of the gas thread during break-up: these mechanisms differed primarily by the process in which the gas thread collapsed in the throat and/or orifice. Dynamic self-assembly of bidisperse bubbles led to unexpected groupings of bubbles during their flow along the outlet channel.

Introduction

This paper describes the stable formation of trains of mono-, bi- and tri-disperse bubbles in microfluidic flow-focusing (FF) junctions. The simplest and most extensively studied structure of a FF junction incorporates a narrow, straight junction (the "orifice"; Figure 1) where the continuous thread of fluid breaks, and bubbles or droplets form[1]. We explored the break-up of the gas thread, and the formation of bubbles, in modified FF geometries in which we replaced the simple orifice with multiple rectangular sections (Figure 1). Each rectangular section can act as a distinct site at which bubbles can form; simple modifications of the geometry of the FF junctions made it possible to generate bi- or tridisperse bubbles (e.g. regular patterns of bubbles of two or three distinct sizes), and complex patterns of bubbles, reproducibly. The dynamics of flow that produced these patterns was too complex for us to model predicatively, but we visualized the different patterns of bubbles that formed at each section in the junction, and inferred mechanisms of formation of bubbles from these visualizations. The streams of multidisperse bubbles generated in these junctions displayed complex interactions as they flowed downstream in the straight outlet channel; the bubbles eventually formed stable, ordered patterns via dynamic self-assembly through the patterns of flow created by the bubbles.

Bubbles and droplets in microfluidics. Multiphase flows are becoming an important part of applied microfluidics. Bubbles, droplets, and complex emulsions are useful in a range of applications, including syntheses of particles[2], crystallization of proteins[3, 4], mixing[5, 6], modulation of light[7], encapsulation of particles and cells[8, 9] and information processing[10, 11]. Among many methods to generate emulsions[12-16], two

types of structures for the generation of bubbles and droplets have proved especially useful; one is the T-junction first described by Thorsen[17], and the other is the flow-focusing junction pioneered by Gañán-Calvo et al. for gas bubbles[18], and by Anna et al. for liquid droplets[1].

The formation of bubbles and droplets takes place via different mechanisms in T-junctions and FF junctions. Both T-junctions[5, 17, 19, 20] and for FF junctions[1, 3, 18, 21] have been explored. The FF system demonstrated the greatest flexibility in control over the size, volume fraction, and structure of the emulsions that it generates. One of the most useful characteristics of the FF systems is their capability to generate monodisperse particles (polydispersity index; $\sigma < 2$ %).[3]

Simple modifications of the geometry of the FF junction can add substantial complexity to the processes that generate bubbles. In this work, our aim was to identify the variables—the geometry of the junction, and the flows of liquid and gas—that influenced the mechanisms that form bubbles. Understanding the formation of emulsions in microfluidic devices has the potential to be useful in applied microfluidics in biology, chemistry[22], and particle synthesis[23].

The formation of bubbles and droplets also represents an interesting set of complex nonlinear behaviors. Unexpected behaviors can arise from the processes that form bubbles and droplets, and the interaction among these bubbles and the flowing liquid[24, 25]. We believe that microfluidic bubble generators will be useful in studying complexity for three reasons: i) the mechanism by which a *simple* generator operates is well-characterized[21]; ii) it is easy to fabricate and modify the structure of these generators by soft lithography[26]; (iii) it is possible to use them to create a large number

of simple components—bubbles and droplets—and to observe the collective behaviors that emerge from their interactions. The study described here demonstrates the use of microfluidic flow-focusing junctions as a testbed with which to explore the unexpected dynamics associated with the formation of bubbles. We rationalize the mechanisms of break-up of the gaseous thread, and formation of bubbles, based on the well-characterized mechanism of formation of monodisperse bubbles, and extend these rationalizations to the generation of bidisperse and tridisperse sets of bubbles.

Experimental Design

Geometry of the Orifice and the Dynamics of Break-up of Bubbles. In a flow-focusing junction, the processes responsible for the generation of bubbles occur primarily in the junction; modification of the geometry of the junction can cause the system to operate in unexpected ways. We have, for example, previously reported stable, long-period oscillatory behavior in the formation of bubbles in multiple FF junctions placed in the channel serially[24], and synchronization of the timing of break-up of threads of gas in multiple FF junction placed in parallel[27].

Briefly, a simple flow-focusing junction (Figure 1a-i) consists of one inlet in the center for the dispersed phase (here, nitrogen gas), and two inlets that connect perpendicularly to the inlet of the dispersed phase for the continuous phase (here, an aqueous solution of Tween 20, 2% w/w). The three streams of fluids meet in the junction, where the dispersed fluid periodically breaks off in the continuous streams and generate bubbles. The study described here modified the geometry of the previously described FF junctions. In this modified design (Figure 1a-ii), the junction became narrower in steps

from upstream to downstream (in contrast to the standard flow-focusing devices[1, 3]). We called the section with the greater width a *throat*, and the section with the smaller width an *orifice*, in order to distinguish the two sections; correspondingly, we referred to this type of FF junction as a "two-section flow-focusing junction." The *throat* section served as another site (in addition to an *orifice*) where the break-up of the thread of gas could occur.

This small modification of the geometry resulted in unexpected changes in the dynamics of the formation of bubbles. The objective of this research was to investigate i) the influence of flow (i.e. rate of water and applied pressure of nitrogen gas) on the mechanism of the formation of bubbles, ii) the influence of the geometries of the multi-section junction on the mechanism of break-up of bubbles, and iii) the dynamic interaction and formation of patterns of bubbles that resulted. We provide a rationalization for our observations, and develop design principles that allow construction of a device for generating bubbles with desired combination of sizes.

Convention and Nomenclatures

Throughout the manuscript, the descriptors in a square bracket are these: [Δp (the pressure of nitrogen (psi)), Q (the rate of flow of water (mL/hr))].

Results and Discussion

We first describe the processes that form groups of gas bubbles with multiple different discrete sizes in a two-section flow-focusing junction. Preliminary observations suggested that i) the rates of flows of fluids in the system, and ii) the geometry and

physical dimensions of the flow-focusing junction determined—or influenced—the mechanism of break-up of bubbles. We surveyed the effects of those parameters on the mechanism of formation of bubbles, and on the dispersity and patterns of bubbles.

Variation in Parameters of Flow. In this section, we describe the mechanism of formation of bubbles in two-section junctions, in response to changes in the rate of flow of water and the applied pressure of nitrogen. Two flow parameters governed the generation of bubbles in the flow-focusing system: Δp – the pressure drop of nitrogen gas across the flow-focusing system (i.e. the dispersed phase that formed bubbles), and Q – the rate of flow of water (i.e. the continuous phase that served as a bulk media surrounding the bubbles). A previous study of the formation of monodisperse bubbles in a simple flow-focusing geometry has shown that the volume of individual bubbles (V_b) scales as $V_b \propto \Delta p/\mu Q$ [3, 21]. The collapse of the neck occurred in the narrow region where three streams met; the scaling suggested the volume of the bubbles was proportional to the speed of the advance of the thread of gas (Δp) and the time required for the thread of gas to collapse ($1/Q$), for a fixed viscosity of the continuous phase (μ). We did not vary the viscosity of the continuous phase in this study.

This same scaling was, however, not generally applicable in two-section junctions. The collapse of the thread of gas could take place in either throat or orifice, and the interplay of the timing of the collapse of the thread of gas, and the advance of the thread of gas, led to different mechanisms of break-up of bubbles. As the result, the system generated bubbles with different sizes. We observed five patterns of break-up in response to the variation of Δp and Q. We called these five regimes *polydisperse*, *monodisperse(1)*,

bidisperse(1-2), *bidisperse(2-1)*, and *monodisperse(2)*. (The following section outlined our observations for the pattern of formation of bubbles in each of five regimes.) The nomenclature *(1)* denotes collapse of the gas thread or bubble in the *first* section (i.e. throat) and the notation *(2)* denoted the collapse of the gas thread or bubble in the *second* section (i.e. orifice) in the two-section junction; the hyphenated numbers denoted positions and order of the break-up. For example, the notation *bidisperse(2-1)* indicated that the system generated bidisperse set of bubbles, as the result of break-up initially in the *second* section (i.e. orifice, or *2*), and subsequently in the *first* section (i.e. throat, or *1*).

Polydisperse: In this regime, the system generated polydisperse bubbles (Figure 2b (i)). We observed this regime at a low rate of flow (Q (mL/hr) ~ 0.25) across a wide range of applied pressure of nitrogen (p). The position of the pinch-off of the thread of gas seemed to be random; we observed the gas thread to retract entirely out of the FF junction, and also to remain in the throat and produce a burst of bubbles. This behavior resulted from a relatively low rate of flow of continuous phase and dispersed phase. For each measurement, we waited three minutes after changing the flow parameters; the system did not exhibit any periodic behavior unlike other regimes described below.

Monodisperse(2): In this regime, the break-up of the thread of gas took place only in the orifice during each cycle of the formation of bubbles. The thread of nitrogen gas remained elongated to the orifice, and always collapsed in the orifice (Figure 2b (ii): t = 1 ms). During each cycle, after each pinch-off, the thread of gas retracted slightly but remained elongated across the throat, and broke up again in the orifice. A low rate of

flow of continuous phase allowed the thread to extend through the throat without collapse. This cycle led to the formation of monodisperse bubbles. We observed this type of break-up at relatively low rates of flow (Q (mL/hr) ~ 0.25) and high pressures of gas ($3.5 \leq p$ (psi) ≤ 4.5).

Bidisperse(2-1): At intermediate rates of flow (Q (mL/hr) ~ 1.0 ms), the system generated bidisperse sets of bubbles across a wide range of applied pressures of gas ($2.5 \leq p$ (psi) ≤ 5.5). Each cycle involved two distinct break-up events, and generated two bubbles with different sizes. At relatively low rates of flow, the thread of gas broke up in the orifice first (Figure 2b (iii): t = 1 ms); after the first break-up, the second break-up occurred in the throat (Figure 2b (iii): t = 25 ms).

Bidisperse(1-2): Upon increasing the rate of flow of continuous phase, the system exhibited a different mechanism for the formation of bidisperse set of bubbles; in this mechanism, the first break-up occurred in the throat to form a bubble; we refer to the bubble formed in this cycle as a mother bubble (Figure 2b (iv): t = 0.5 ms). The mother bubble broke up again into two bubbles while travelling in the orifice (Figure 2b (iv): t = 2.5 ms). While the mother bubble traveled through the orifice, a large volume fraction of the bubble remained in the throat; the mother bubble itself blocked the orifice, and the stream of the continuous phase caused the second break-up by pinching off the tail of the mother bubble; we referred to the two bubbles formed in this cycle as daughter bubbles.

Monodisperse(1): At an even higher rate of flow of continuous phase (Q (mL/hr) > 2.0), the system generated monodisperse bubbles (Figure 2b (v)). The break-up of the thread took place exclusively in the throat. The bubble generated in the throat passed through the orifice to the outlet channel without further break-up events.

In summary, the thread of gas could collapse either in the throat or the orifice, depending on the flow parameters. The locations of the break-up of the gas thread, and the resulting sizes of bubbles led to the formation of different patterns of monodisperse, bidisperse or polydisperse bubbles.

Transition between Different Mechanisms of Break-up. Variation in the flow parameters induced different patterns of bubbles, by changing the positions of the thread of gas at which pinch-off took place. These examinations suggested that initial break-up took place in the throat (i.e. the first section) at relatively high rates of flow, and in the orifice (i.e. the second section) at relatively low rates of flow. The observation could be rationalized by considering the relative significance of three timescales; i) the time required for the collapse of the thread in the throat (τ_{throat}); ii) the time required for the collapse of the thread in the orifice ($\tau_{orifice}$); and iii) the time required for the thread to advance from the throat to the orifice ($\tau_{advance}$).

The initial break-up took place in the throat when either Eqn 1 or Eqn 1' described the system:

$$\tau_{throat} < \tau_{advance} + \tau_{orifice} \quad (1)$$

$$\tau_{throat} - \tau_{orifice} < \tau_{advance} \quad (1')$$

On the other hand, the initial break-up took place in the orifice when either Eqn 2 or Eqn 2' described the system:

$$\tau_{throat} > \tau_{advance} + \tau_{orifice} \quad (2)$$

$$\tau_{throat} - \tau_{orifice} > \tau_{advance} \quad (2')$$

A previous study of the flow-focusing generator[21] indicated that the quantity on the left side of Eqn 1' and Eqn 2', $\tau_{throat} - \tau_{orifice}$, was a function of the width of the throat and orifice (w_1 and w_2) and of the volumetric flow rate of continuous phase (Q) (i.e. the width of the thread of gas and the rate at which it collapsed.) For a fixed geometry, this quantity decreased with Q, and consequently the speed of the collapse increased. The other quantity, $\tau_{advance}$, was the time required for the thread of gas to move through the orifice, and was a function of the length of the throat (l_1) and the applied pressure of nitrogen (Δp) (i.e. the speed of the advance of the thread of gas, and the distance it travelled); at higher values of Δp, the time required for the thread of gas to advance through a given distance of the throat (l_1) decreased. We therefore expected that the initial break-up would occur in the throat at higher values of Q and lower values of Δp (this expectation agreed with the data described in Figure 2).

In addition, the decrease in the size of bubbles rationalized the transition from *bidisperse(1-2)* to *monodisperse(1)* at higher values of Q. The scaling for the volume of bubbles, $V_b \propto \Delta p/\mu Q$, (with μ fixed in this study) should apply to a simple flow-focusing geometry (Figure 1a, i); the generator thus formed smaller bubbles at higher values of Q. Bubbles that were sufficiently small escaped into the outlet channel without experiencing a second break-up, and the presence of the orifice did not cause any change in the pattern of the break-up. This process generated monodisperse bubbles.

The examination of the influence of the flow parameters suggested that that the interplay of the timing of the break-up in the throat and the orifice led to different

mechanisms. We hypothesized that it would also be possible to control the timing and order of the break-up by changing the *geometry* of the junction.

Variation in Physical Dimensions of the Junction. We investigated the influence of the dimensions of the junction (that is the geometry of the *orifice* and *throat*) on the mechanism of generation of bubbles. In the following, we describe and rationalize the patterns of the break-up we observed. We also demonstrate that a more complex geometry of the junction—a junction with three different sections for break-up—could generate tridisperse bubbles reproducibly.

Length of the Throat (l_1). We first explored the influence of variations in the length of the throat (l_1) on the performance of the two-section flow-focusing junction. The hypothesis was that the length of the throat (l_1) would alter the position of the break-up of the thread of gas by changing the time required for the gas thread to advance through the throat ($\tau_{advance}$; the parameter on the right-hand side of Eqn 1' and Eqn 2'). Changes in l_1 alone (with *p* and *Q* held constant) were sufficient to cause the formation of bubbles to occur in three different mechanisms (*bidisperse(1-2)*, *bidisperse(2-1)*, and *monodisperse(2)*, Figure 3). For the longest l_1 (= 400 μm), the break-up was by *bidisperse(1-2)*. For intermediate l_1 (= 200 ~ 300 μm), the break-up pattern was *bidisperse(2-1)*. For small l_1 (= 100), the break-up was by *monodisperse(2)*.

The relative significance of different time-scales (represented by τ_{throat}, $\tau_{orifice}$, and $\tau_{advance}$) rationalized the transition of the mechanism for the break-up. The previous section suggested that the initial break-up took place in the throat if $\tau_{throat} - \tau_{orifice}, <$

$\tau_{advance}$, and took place in the orifice if $\tau_{throat} - \tau_{orifice}, > \tau_{advance}$ (Eqn 1' and Eqn 2'). The quantity on the left-hand side of the equation (i.e. $\tau_{throat} - \tau_{orifice}$) was largely constant because we did not change the speed of the continuous phase (and hence the speed of collapse of the gas thread). The parameter on the right-hand side ($\tau_{advance}$: the time required for the thread of the gas to advance through the throat) depended on the length of the throat. A longer throat would require more time for the gas thread to travel through, and we therefore expected the initial break-up to occur in the throat, if the throat were longer.

Our observation supported this hypothesis: the longest throat we examined (or equivalently, the largest $\tau_{advance}$) caused the thread to break in the throat (Figure 3a). When the length of the throat decreased sufficiently, the break-up took place in the orifice (Figure 3d). We considered two asymptotic cases to rationalize how the variation of l_1 influenced the mechanism of the break-up, for a fixed set of flow parameters; $l_1 = 0$ and $l_1 = \infty$. The former would result in the break-up of the thread in the *orifice* (since the throat would not exist in such a system), while the latter would result in the break-up in the *throat* (since the length of the throat would be infinite.) We thus anticipated that there existed a critical length of the throat (l_1^*) for which the location of the *first* break-up switches from the orifice to the throat. The white arrows on the right column of images in Figure 3 indicated the positions of the thread at which initial collapse occurred. For the values of p and Q that we applied in this study, l_1^* lay between 300 μm and 400 μm. We note that for an intermediate length of throat (Figure 3b; $l_1 = 300$), the *second* collapse initiated in the throat during the *first* break-up in the orifice. The emergence of the second point of collapse in the neck, before the completion of the first break-up, allowed less

time for the second bubbles to grow, and thus generated small second bubbles (Figure 3b). As the length of the throat was made shorter (Figure 3c), the difference in the size of the two bubbles also became smaller.

Width of the Orifice (w_2). The width of the orifice (w_2) changed the time required for the break-up of the mother bubbles in the orifice, and therefore the timing of a possible second break-up of a bubble as it passed through the orifice. We observed pronounced changes in the second break-up that formed the daughter bubbles, when the system generated bubbles in the *bidisperse(1-2)* regime.

We varied the width of the orifice, and observed the change in the size of daughter bubbles that formed during the second break-up. Figure 4 showed optical micrographs of arrays of bubbles generated in two-section junctions. The images showed a correlation between the widths of the orifice and the size of the rear daughter bubbles (i.e. the smaller bubble in each pair in this example) in the *bidisperse(1-2)* regime for a fixed set of flow-parameters; the rear daughter bubble was larger when the width of the orifice was smaller. Said otherwise, the smaller the width of the orifice, the larger the fraction of mother bubbles that remained in the throat during the second break-up in the orifice. (Note that the smaller bubble passed the larger bubble, settled in the front of the larger bubble, and the two bubbles flowed together downstream as one assembly (Figure 4d). We described the details of this process in a later section and in Figure 7.)

The time required for the collapse of the (mother) bubbles in the orifice ($\tau_{orifice}$) depended on 1) the speed of flow of water that induced collapse in the orifice, and 2) the width of the neck of a bubble that collapsed in the orifice. The narrower the orifice, the higher the speed of collapse; for a constant volumetric flow, the local speed of the fluid in

the *orifice* area—and equivalently, the speed of collapse of the mother bubble—was higher for narrower orifices than for wider orifices. In addition, the width of the orifice was roughly equal to the width of the neck of the bubble that collapsed, because the bubble spanned the entire width of the channel when it first entered the orifice. Therefore, the decrease in the width of the orifice caused these two parameters to change in a way that decreased $\tau_{orifice}$ and increased the size of the rear daughter bubbles.

Length of the Orifice (l_2). The length of the orifice determined the time required for a bubble to travel through the orifice; the orifice needed to have a minimum length, for the mother bubble to collapse and produce two daughter bubbles while it flowed through the orifice. We studied the formation of the daughter bubbles in the orifice (a *bidisperse(1-2)* regime), and used a sufficiently long throat ($l_1 = 400$) to ensure that the initial break-up occurred in the throat (as described in the previous section that discussed the influence of l_1 on the formation of bubbles.)

Experimental observations supported our hypothesis; for short lengths of the orifice (Figure 5a, 5b and 5c; $l_2 = 25 \sim 75$ μm), the systems generated arrays of monodisperse bubbles. The pattern was *monodisperse(1)*. For long orifices (Figure 5d and 5e; $l_2 = 100 \sim 150$ μm), the second break-up took place in a way that generated *bidisperse(1-2)* bubbles. These experiments demonstrated that it was possible to design the channel to generate either monodisperse or bidisperse bubbles simply by changing the length of the orifice.

Three-section Junction. We explored whether more complex shapes of junctions—specifically shapes comprising three sections—would provide additional sites for break-up of bubbles. We tested a flow-focusing junction comprising three rectangular

sections (which we call a three-section flow-focusing junction). We refer to the three sections as *first*, *second*, and *third*, moving from upstream to downstream (Figure 6).

The three-section flow-focusing junction provided three sites at which a thread of gas could break (Figure 6a and 6b), and generated regular sequence of bubbles of three sizes. Figure 6c shows time-resolved images for the progression of the break-up; the break-up pattern was (following the convention used throughout the manuscript) *tridisperse(3-1-2)*. Complete characterization of this junction would be much more complex than that for the simpler systems; three patterns of monodisperse break-up (i.e. *1, 2* or *3*), six patterns of bidisperse break-up (i.e. *1-2, 2-1, 1-3, 3-1, 2-3* or *3-2*) and six patterns of tridisperse break-up (*1-2-3, 1-3-2, 2-1-3, 2-3-1, 3-1-2* or *3-2-1*) would, in principle, be possible (considering all the permutations). In addition, two different events of bidisperse break-up could take place in one cycle (for example, both *bidisperse 1-3* and *bidisperse 2-3* might take place in one cycle). We have not completely characterized this system, but we believe that design principles inferred from a two-section junction will be applicable to the design of systems to generate bubbles with higher dispersity. For example, the observation that 1) an increase in a length of a given section facilitated the formation of bubbles in that section, and 2) an increase in a width of a given section increased the time required for the break-up in the section, should still hold for a system with a flow-focusing junction comprising multiple sections.

Dynamic Pattern Formation in Multidisperse Bubbles. Another interesting phenomenon in these systems was dynamic self-assembly of patterns of bubbles (Figure 7). Previous studies of formation of patterns of emulsions includes formation of regular

arrays of monodisperse bubbles[17, 18], composite lattices of bubbles and droplets[28], arrays of non-spherical droplets[29, 30], and fluctuating one-dimensional array of bubbles[25]. Here, we observed dynamic self-assembly of multidisperse bubbles into clusters while flowing down the outlet channel. Depending on the size of a large bubble relative to the width of the channel, however, the smaller bubble took different paths in reaching a stable position with respect to the larger bubble.

Larger bubbles experience higher flow resistance (i.e. feel higher drag) than smaller bubbles[31], and thus flow more slowly in a continuous medium; the largest bubbles traveled at the slowest speed in these systems. In an observation frame that moved at the velocity of flow of the largest bubbles, the continuous phase would be considered as a flow passing periodic circular cylinders (i.e. these large bubbles). In Figure 7b and 7c, smaller bubbles readily deviated from the center of the flow along the extensional flows created by the large bubbles. Over the range of Reynolds numbers under which these experiments were conducted ($Re = \rho vd/\mu \sim 2$, with $\rho = 1$ g/cm^3, $v = 10$ μm/ms, $d = 200$ μm, and $\mu = 1$ g/m-s), flows past a cylinder start to separate and create recalculating eddies in front of the cylinder[32]. These eddies trapped the smaller bubbles in front of the larger bubbles.

The larger bubbles entered the outlet channel first, and the smaller one then followed. We observed two different processes of assembly: i) the smaller bubble was captured by the *next* (following) larger bubble (Figure 7a), and ii) the smaller bubbles passed the side of the larger bubbles, along the extensional fields of flows, and eventually settled in front of the largest bubble. (Figure 7b and 7c) Two or three bubbles associated in a similar way as they flowed in the channel. We believe that three major factors

determined the process followed by self-assembly: i) the velocity of the flow of bubbles and continuous phase, ii) the size of small and large bubbles, and iii) the width of the outlet channel. These three variables influenced the fluidic resistance, and thus the velocities of flows, associated with the two pathways for assembly (i.e. association of a small bubble with a larger bubble in the front or in the back), and determined the direction of the flow of the small bubbles.

The velocity of flows, and the size of the bubbles were not *independent*, however, and it was not possible to decouple these two variables in our system. In addition, the fluidic resistance of a given path changed dynamically as the position of bubbles, and their position relative to the wall of the channel, changed over time. For example, while the small bubble was flowing through a region defined by the large bubble and the wall, the fluidic resistance of the path increased and the velocity of the flow decreased. These characteristics of the system made it difficult to understand the details of the processes involved in the assembly of the bubbles analytically.

Conclusions

This paper described formation of bubbles in a flow-focusing junction comprising multiple rectangular sections in the bubble-forming region. We surveyed the flow parameters, and the geometries of the flow-focusing junction, for their influences on the mechanisms that formed bubbles. Our demonstrations suggest that it will be possible to design flow-focusing junctions to generate monodisperse, bidisperse, and tridisperse sets of bubbles; Formation of bubbles can, in principle and in practice, occur at any one of the rectangular sections in the junction, and the location and order of formation of bubbles

determined the size and dispersity of bubbles that the junction generated in each cycle. Our study demonstrates that appropriate designs of the flow-focusing junction can control the dynamics of break-up of the thread of gas, and the patterns of bubbles that resulted.

Study for Complexity and Emergent Behaviors. This work provides examples of complex and emergent behaviors generated by *synthetic* approaches[21, 27]. *Interactions* of the multiple elements (i.e. multiple flow-focusing sections and multiple bubbles generated in them) resulted in the complex behaviors observed. Flow-focusing junctions can be fabricated easily using soft lithography, and these junctions can serve as a useful platform for the exploration of complex behaviors in systems that generate bubbles and droplets. In previous work, we observed that relatively simple behaviors suddenly became complex when multiple generators were allowed to interact[21, 27]. Many of these complex behaviors could be rationalized retrospectively and qualitatively, but not (yet) predicted analytically. Qualitative information, however, may provide useful insight into the overall behavior of the system, and allow us to identify the most important interaction. We infer that the interactions between the processes that form bubbles in each section can be determined by the geometries of these sections. The observations also suggest simple design principles for more complex flow-focusing systems comprising multiple sections. We believe that this type of constructionist—in contrast to reductionist—approach (i.e. building complex systems from a well-characterized, simple components) should also provide information useful in understanding, and eventually fabricating, complex systems with desired functionality.

Experimental

Fabrication of the device. We fabricated the channel system for the microfluidic devices in poly(dimethylsiloxane) (PDMS) slabs using soft lithography, and sealed these slab to a glass cover slide (Corning) using plasma oxidation[26, 33].

Microfluidics. Immediately after sealing the device, we filled the channel of PDMS with the aqueous solution of Tween 20 surfactant (2% w/w; the continuous phase used for the experiment) to ensure that the walls of the microchannels remained hydrophilic. Nitrogen was the dispersed phase. A digitally controlled syringe pump (Harvard Apparatus, PhD2000 series) delivered the continuous phase to the device at a specified rate of flow. A pressurized tank provided the microfluidic device with gas at constant pressure via a needle valve and a digital manometer (Omega). Polyethylene tubing (PE60, Becton Dickinson) connected between the source of the fluid and the PDMS microfluidic channels.

Imaging. A Phantom V9 fast camera and a Nikon objective recorded still images and videos of the image of bubbles. A Leica microscope and the same camera acquired movies and images of the flowing arrays of bubbles.

Acknowledgements

This material is based on work supported by the Department of Energy under award number DE-FG02-00ER45852**.** We thank Professor Howard Stone for insightful discussions.

References

[1] S. L. Anna, N. Bontoux, H. A. Stone, *Appl. Phys. Lett.* **2003**, *82*, 364.

[2] S. Q. Xu, Z. H. Nie, M. Seo, P. Lewis, E. Kumacheva, H. A. Stone, P. Garstecki, D. B. Weibel, I. Gitlin, G. M. Whitesides, *Angew. Chem. Int. Ed.* **2005**, *44*, 724.

[3] P. Garstecki, I. Gitlin, W. DiLuzio, G. M. Whitesides, E. Kumacheva, H. A. Stone, *Appl. Phys. Lett.* **2004**, *85*, 2649.

[4] J.-u. Shim, G. Cristobal, D. R. Link, T. Thorsen, Y. Jia, K. Piattelli, S. Fraden, *J. Am. Chem. Soc.* **2007**, *129*, 8825.

[5] J. D. Tice, H. Song, A. D. Lyon, R. F. Ismagilov, *Langmuir* **2003**, *19*, 9127.

[6] P. Garstecki, M. J. Fuerstman, M. A. Fischbach, S. K. Sia, G. M. Whitesides, *Lab Chip* **2006**, *6*, 207.

[7] M. Hashimoto, B. Mayers, P. Garstecki, G. M. Whitesides, *Small* **2006**, *2*, 1292.

[8] S. Takeuchi, P. Garstecki, D. B. Weibel, G. M. Whitesides, *Adv. Mater.* **2005**, *17*, 1067.

[9] A. Huebner, M. Srisa-Art, D. Holt, C. Abell, F. Hollfelder, A. J. deMello, J. B. Edel, *Chem. Commun.* **2007**, 1218.

[10] M. J. Fuerstman, P. Garstecki, G. M. Whitesides, *Science* **2007**, *315*, 828.

[11] M. Prakash, N. Gershenfeld, *Science* **2007**, *315*, 832.

[12] J. M. Gordillo, Z. D. Cheng, A. M. Ganan-Calvo, M. Marquez, D. A. Weitz, *Phys. Fluids* **2004**, *16*, 2828.

[13] Q. Y. Xu, M. Nakajima, *Appl. Phys. Lett.* **2004**, *85*, 3726.

[14] D. R. Link, S. L. Anna, D. A. Weitz, H. A. Stone, *Phys. Rev. Lett.* **2004**, *92*.

[15] S. Okushima, T. Nisisako, T. Torii, T. Higuchi, *Langmuir* **2004**, *20*, 9905.

[16] A. S. Utada, E. Lorenceau, D. R. Link, P. D. Kaplan, H. A. Stone, D. A. Weitz, *Science* **2005**, *308*, 537.

[17] T. Thorsen, R. W. Roberts, F. H. Arnold, S. R. Quake, *Phys. Rev. Lett.* **2001**, *86*, 4163.

[18] A. M. Gañán-Calvo, J. M. Gordillo, *Phys. Rev. Lett.* **2001**, *87*.

[19] T. Nisisako, T. Torii, T. Higuchi, *Lab Chip* **2002**, *2*, 24.

[20] P. Garstecki, M. J. Fuerstman, H. A. Stone, G. M. Whitesides, *Lab Chip* **2006**, *6*, 437.

[21] P. Garstecki, H. A. Stone, G. M. Whitesides, *Phys. Rev. Lett.* **2005**, *94*.

[22] H. Song, D. L. Chen, R. F. Ismagilov, *Angew. Chem. Int. Ed.* **2006**, *45*, 7336.

[23] R. K. Shah, H. C. Shum, A. C. Rowat, D. Lee, J. J. Agresti, A. S. Utada, L.-Y. Chu, J.-W. Kim, A. Fernandez-Nieves, C. J. Martinez, D. A. Weitz, *Mater. Today* **2008**, *11*, 18.

[24] P. Garstecki, M. J. Fuerstman, G. M. Whitesides, *Nat. Phys.* **2005**, *1*, 168.

[25] T. Beatus, T. Tlusty, R. Bar-Ziv, *Nat. Phys.* **2006**, *2*, 743.

[26] D. C. Duffy, J. C. McDonald, O. J. A. Schueller, G. M. Whitesides, *Anal. Chem.* **1998**, *70*, 4974.

[27] M. Hashimoto, S. S. Shevkoplyas, B. Zasonska, T. Szymborski, P. Garstecki, G. M. Whitesides, *Small* **2008**, *4*, 1795.

[28] M. Hashimoto, P. Garstecki, G. M. Whitesides, *Small* **2007**, *3*, 1792.

[29] M. Hashimoto, P. Garstecki, H. A. Stone, G. M. Whitesides, *Soft Matter* **2008**, *4*, 1403.

[30] M. Seo, C. Paquet, Z. Nie, S. Xu, E. Kumacheva, *Soft Matter* **2007**, *3*, 986.

[31] H. Wong, C. J. Radke, S. Morris, *J. Fluid Mech.* **1995**, *292*, 95.

[32] M. V. Dyke, *Album of Fluid Motion*, 1st ed., The Parabolic Press, Stanford, **1982**.

[33] Y. N. Xia, G. M. Whitesides, *Annu. Rev. Mater. Sci.* **1998**, *28*, 153.

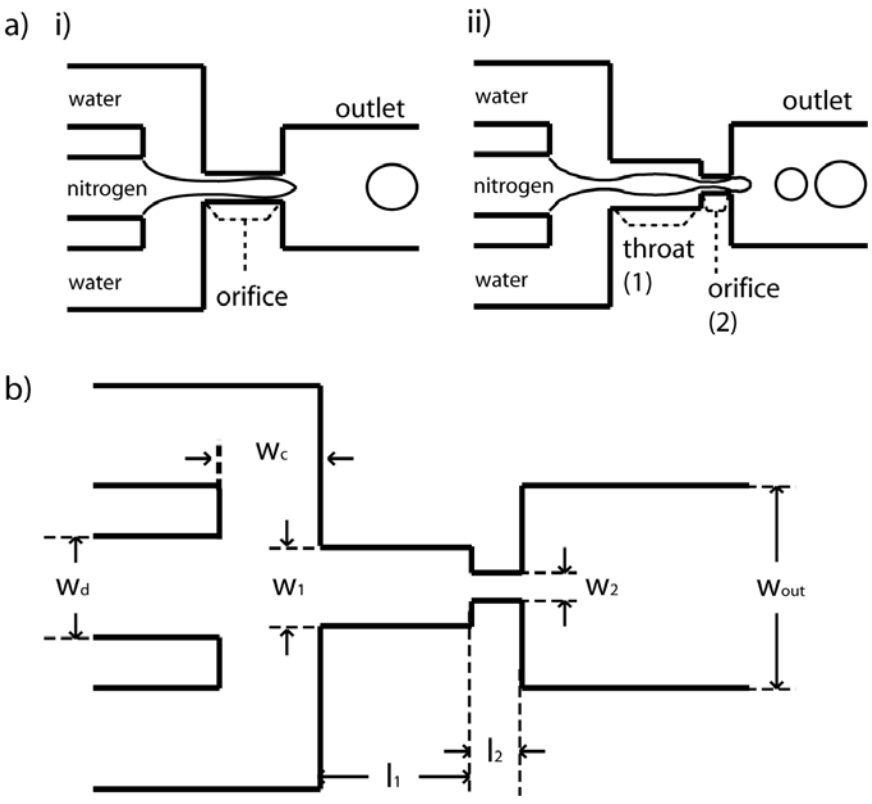

Figure 1. a) Schematic illustration of the flow-focusing junction and definition of the throat and orifice; i) a simple flow-focusing junction, and ii) a multi-width flow-focusing junction. **b)** Definition of the parameters describing the geometry of the channel. The width and length of the throat are w_1 and l_1, respectively, and the width and the length of the orifice are w_2 and l_2, respectively. Other parameters indicated in the figure are the width of the inlet for the dispersed phase (w_d), the width of the inlets for the continuous phase (w_c), and the width of the outlet channel (w_{out}). In this work, the width of the orifice was always smaller than the width of the throat ($w_1 > w_2$).

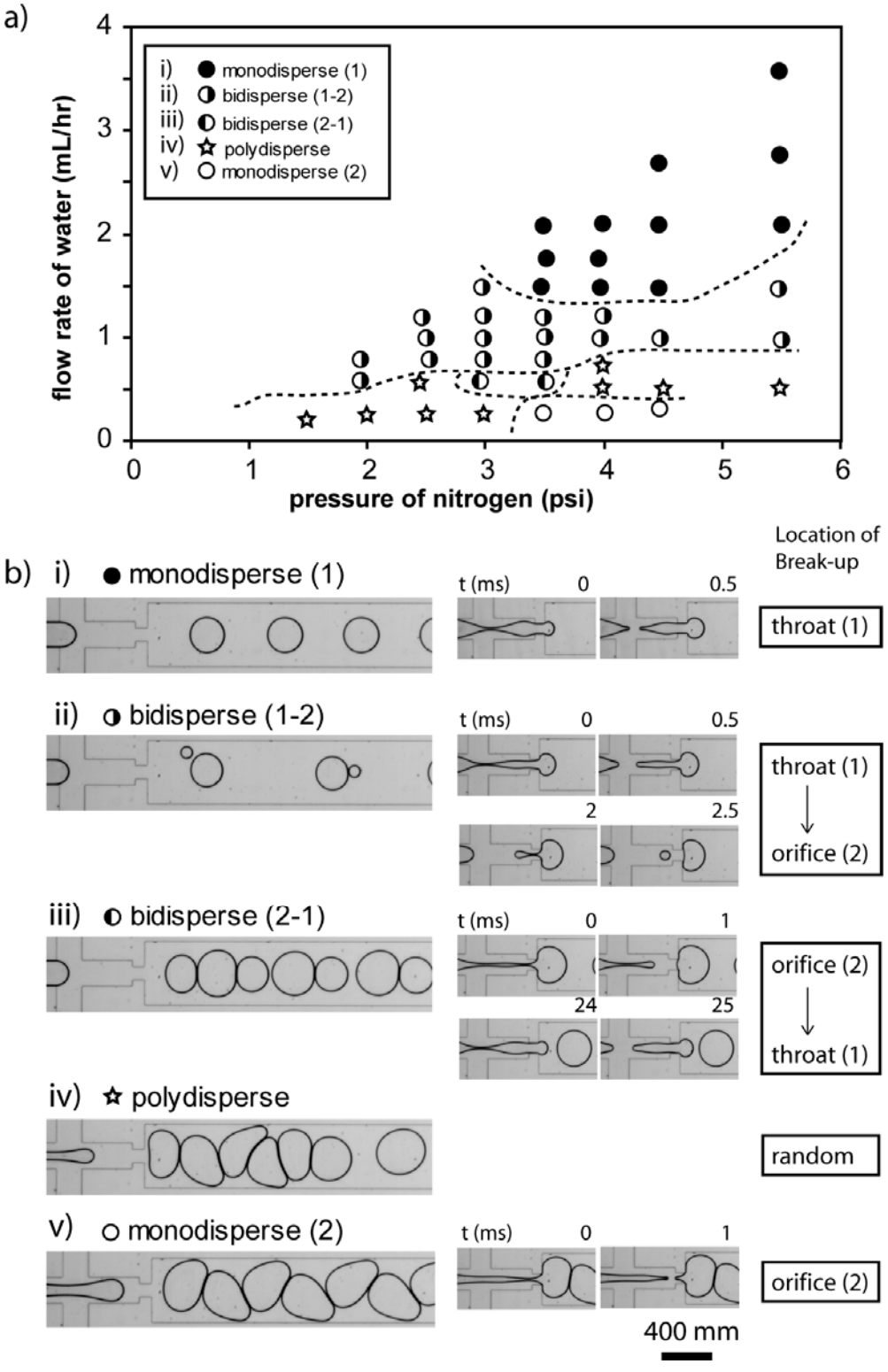
a)
flow rate of water (mL/hr)
pressure of nitrogen (psi)
i) monodisperse (1)
ii) bidisperse (1-2)
iii) bidisperse (2-1)
iv) polydisperse
v) monodisperse (2)
b)
Location of Break-up
i) monodisperse (1)
t (ms) 0 0.5
throat (1)
ii) bidisperse (1-2)
t (ms) 0 0.5
2 2.5
throat (1)
orifice (2)
iii) bidisperse (2-1)
t (ms) 0 1
24 25
orifice (2)
throat (1)
iv) polydisperse
random
v) monodisperse (2)
t (ms) 0 1
orifice (2)
400 mm

Figure 2. a) A phase diagram indicating the mechanism of formation of bubbles as a function of the pressure of nitrogen (dispersed phase) and the rate of flow of water (continous phase). The vertical axis represents *Q*, the rate of flow of water (continuous phase), and the horizontal axis represents Δp, the applied pressure of nitrogen (dispersed phase). The dimensions of the junction (in μm) were $w_1 = 200$, $l_1 = 400$, $w_2 = 100$, and $l_2 = 100$, respectively. **b)** Representative images of the five regimes of break-up indicated by the legend.

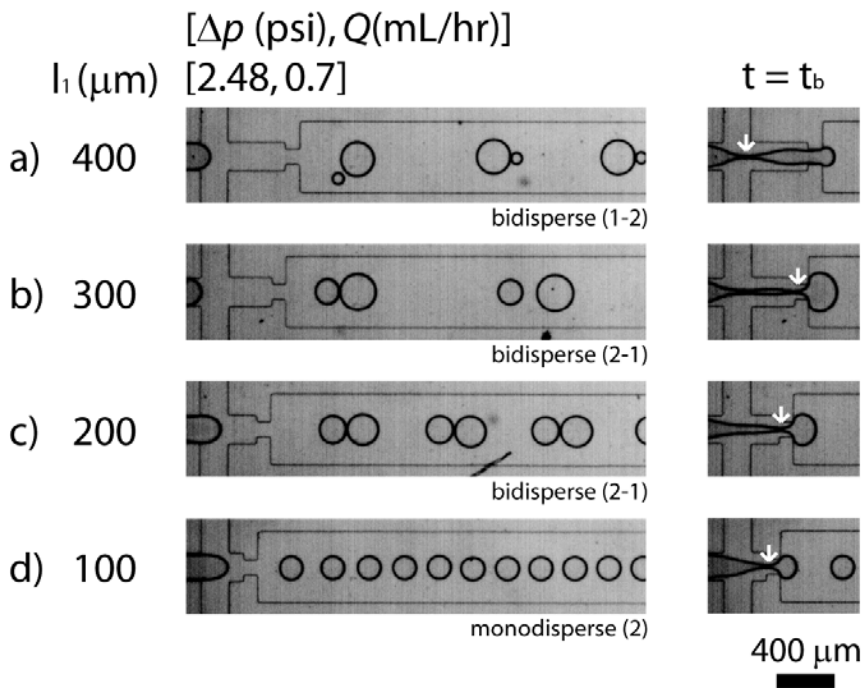

Figure 3. Variation of the length of the throat (l_1), and resulting patterns of bubbles in the outlet channel. The set of images in the right-hand column are instantaneous snapshots of the thread of gas at a time immediately before the first break-up. The break-up occurred in the throat for a), and in the orifice for b) – d). The white arrows superimposed on the images on the right column indicate the position of the *first* break-up of each break-up cycle.

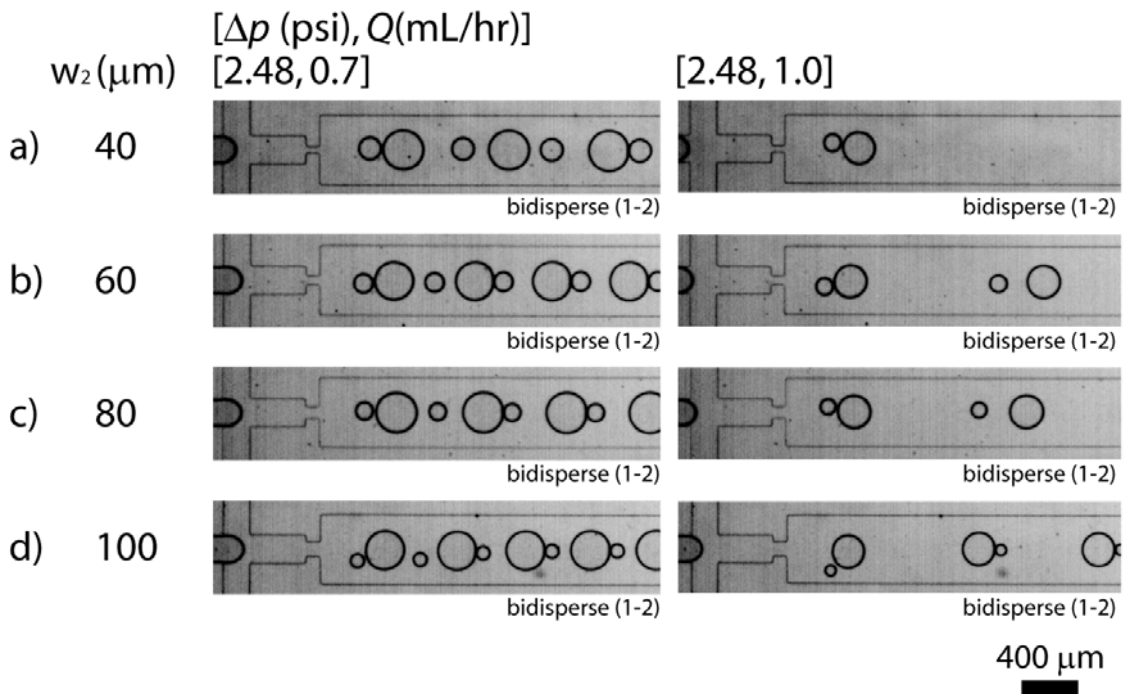

Figure 4. Variations in the width of the orifice (w_2), and resulting patterns of bubbles in the outlet channel.

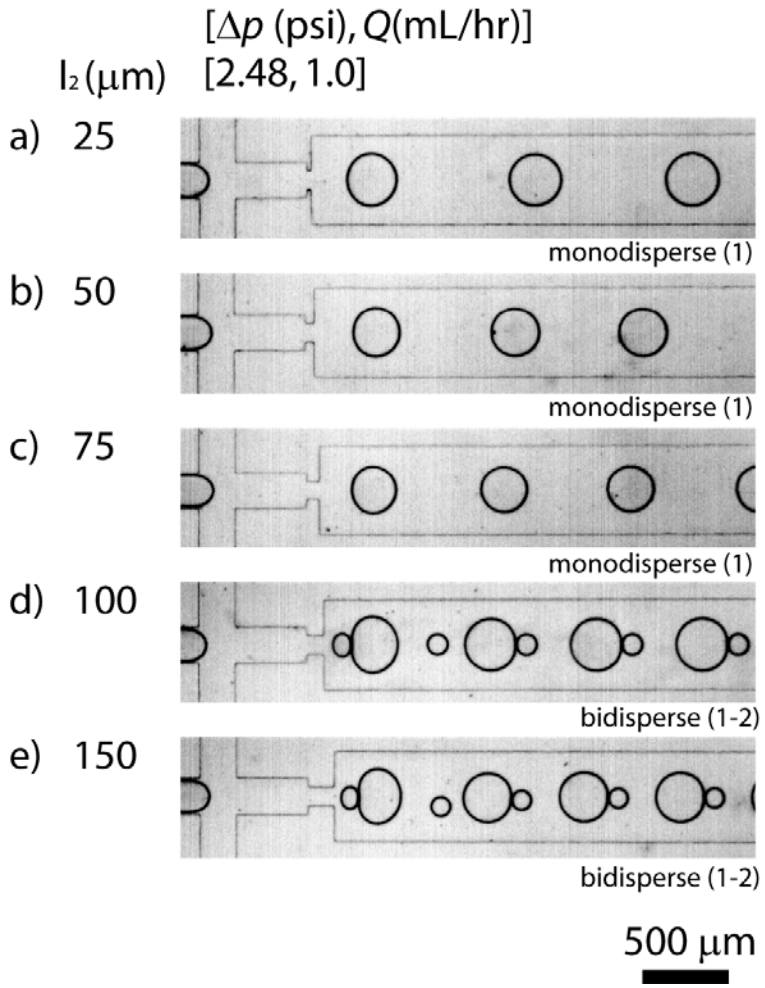

Figure 5. Variation of the length of the orifice (l_2), and resulting patterns of bubbles in the outlet channel.

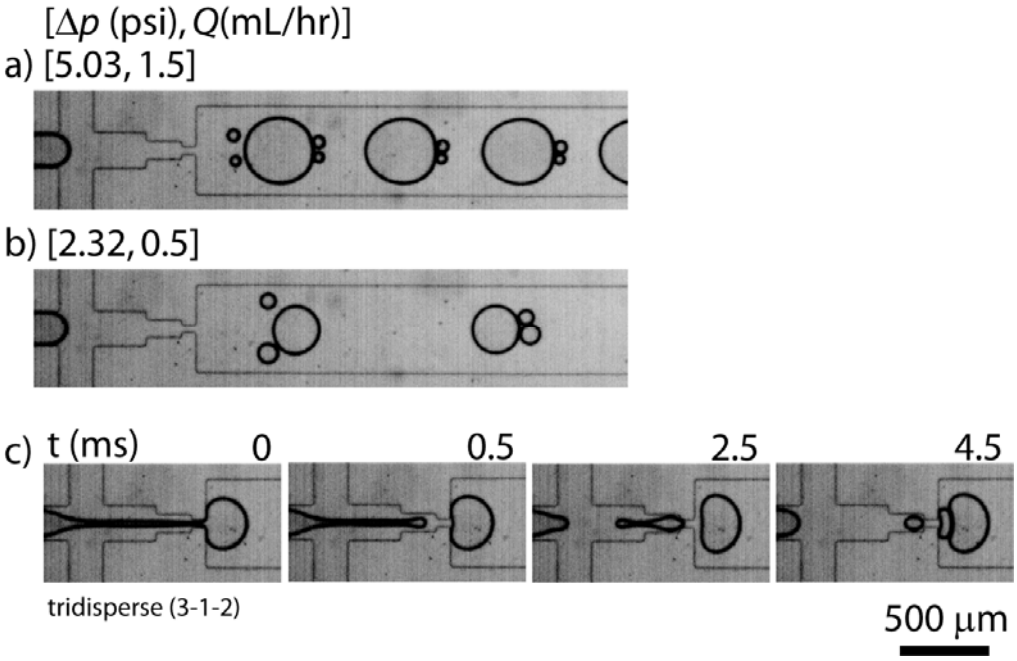

Figure 6. Break-up of the thread of the gas in a three-width orifice. **a)**, **b)** Optical micrographs of tridisperse bubbles formed in the three-width orifice. **c)** Time-resolved optical micrographs of the thread of gas breaking in the three-width flow-focusing orifice. The numbers on the top, right corner of the images indicate elapsed time (t) in millisecond. The time was set to zero in the first image. At t = 0.5, the gas thread broke in section*(3)*. The thread slightly retracted, and broke in section*(1)* at t = 2.5. Finally the daughter bubble from the immediately previous break-up went through another break-up at t = 4.5 in section*(2)*, and thus generated the third bubble.

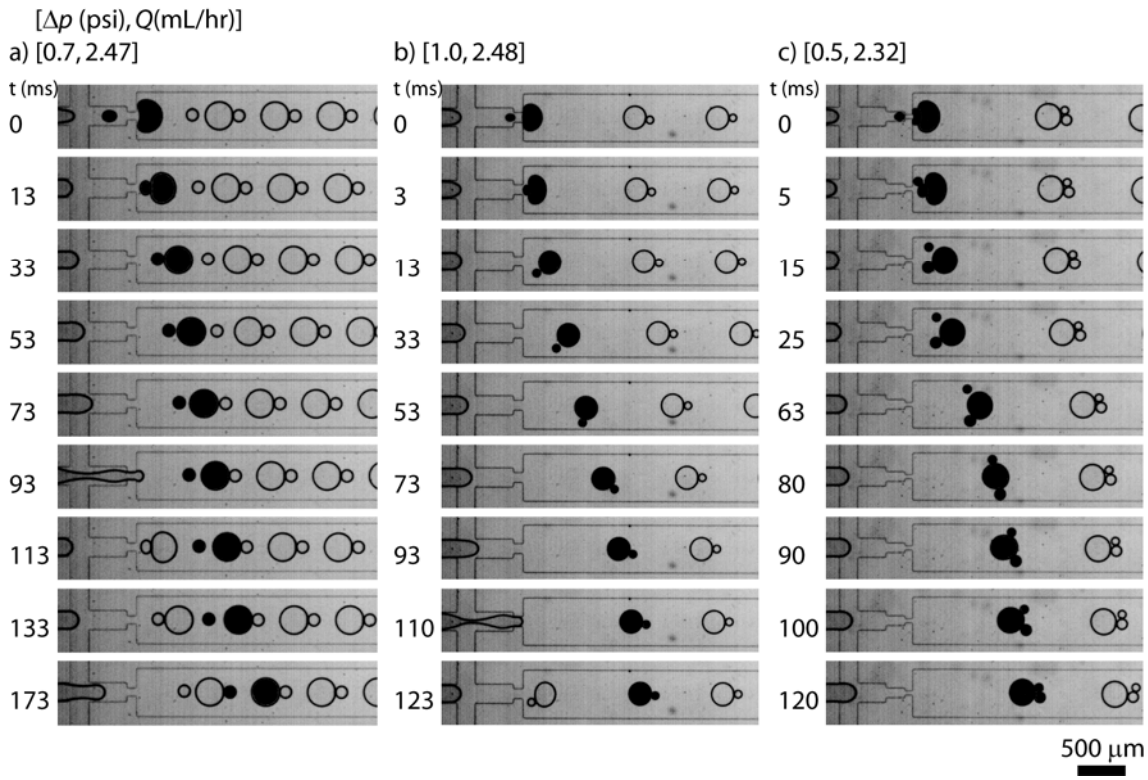

Figure 7. Dynamic self-assembly of bubbles. A single break-up generated one set of bubbles (artificially colored black using Photoshop, for easier interpretation). a) bidisperse bubbles: The larger bubble from one break-up associated with the smaller bubble from the previous break-up, b) bidisperse bubbles: the large and the small bubbles from a single break-up associated in a process which the small bubble flowed along the side of the large bubble, and c) tridisperse bubbles: bubbles of three different sizes from a single break-up associated together as the two smaller bubbles flowed around opposite sides of the largest bubble.